JOURNAL OF GUIDANCE, CONTROL, AND DYNAMICS
Vol. 16, No. 1, January–February 1993

Flight Simulator Fidelity Assessment in a Rotorcraft Lateral Translation Maneuver

R. A. Hess* and T. Malsbury†
University of California, Davis, Davis, California 95616
and
A. Atencio Jr.‡
NASA Ames Research Center, Moffett Field, California 94035

A model-based methodology for assessing flight simulator fidelity in closed-loop fashion is exercised in analyzing a rotorcraft low-altitude maneuver for which flight test and simulation results were available. The addition of a handling qualities sensitivity function to a previously developed model-based assessment criteria allows an analytical comparison of both performance and handling qualities between simulation and flight test. Model predictions regarding the existence of simulator fidelity problems are corroborated by experiment. The modeling approach is used to assess analytically the effects of modifying simulator characteristics on simulator fidelity.

Introduction

FOR reasons of economics and safety, the aerospace community is becoming increasingly reliant on flight simulation as a fundamental tool for both flight control research and pilot training. Confidence in the flight simulator as a valid research and training tool is dependent on the fidelity of the simulator. As used herein, flight simulator fidelity refers to the ability of a simulator to induce adequate pilot psychomotor and cognitive behavior for a given task and environment. An analytical methodology for preliminary assessment of piloted flight simulator fidelity has been presented in Ref. 1. The pilot-model-based methodology was developed using flight and simulation data for two low-speed rotorcraft maneuvers, as reported in Refs. 2 and 3.

Although the same vehicle is used, the flight and simulation experiments to be discussed and analyzed herein represent a different set of experiments than those discussed in Refs. 2 and 3 and used in the modeling effort of Ref. 1. In particular, considerable effort was expended in the design and conduct of the experiment to ensure that the visual cue environments in both flight and simulation were as similar as possible. One important element in accomplishing this similarity was the use of a hover test rig, which will be described.

The fidelity assessment scheme offered in Ref. 1 is based on the supposition that, in any specific task, simulator fidelity problems arise from simulator limitations that adversely affect the pilot's "primary control" loop. The primary control loop is defined by a manual control task modeling procedure that employs sequential feedback loop closures. These closures are similar to those that would be used by a classical control system designer faced with designing an inanimate controller to accomplish the same task as that asked of the pilot. The innermost control loop that results from this task modeling procedure is referred to as the "primary control" loop and involves direct manipulative inputs by the pilot.

As an example, consider Fig. 1, which shows a manual control system consisting of a pair of sequential feedback loops. The pilot compensation is assumed to be contained in elements Yp_1 and Yp_2. Feedback structures such as that of Fig. 1 are often referred to as "single-point, multiloop systems."[4] In either manual or automatic systems, the bandwidths or the cross-over frequencies associated with each loop decrease as one proceeds from inner to outer loop. The primary control loop of Fig. 1 is the loop with "1" subscripted variables. For the rotorcraft lateral translation maneuver that is the subject of this research, variable m_1 in Fig. 1 represents vehicle roll attitude ϕ, m_2 represents lateral translation y, and the pilot manipulative input δ represents lateral cyclic control inputs δ_A.

In the assessment technique offered in Ref. 1, simulator fidelity problems are assumed to exist if, in comparing primary control loops between the actual (nominal) and simulated vehicle, significant differences are found to exist between 1) predicted pilot compensation Yp_1, and/or 2) the bandwidths of the closed, primary-loop transfer function m_1/c_1. In generating Yp_1, and, consequently, m_1/c_1, a relatively simple control theoretic model of the human pilot is employed.

A limitation of the methodology of Ref. 1 lies in the omission of any capabilities for the prediction of handling qualities rating (HQR) differences between nominal and simulated vehicles. This is not an inconsequential omission, as differences in HQR, i.e., Cooper-Harper pilot ratings,[5] between simulation and flight test are often considered prima facie evidence of simulator fidelity problems. Such was the case, for example, in the flight test and simulation results reported in Refs. 2 and 3, where not only did mean HQRs differ for like tasks, but almost no overlap existed *in the range* of the HQR's given by the five evaulation pilots for each task. Thus, the primary contribution of the research to be described is an extension of the methodology of Ref. 1 to include some form of handling qualities prediction.

First described are the flight test and simulation experiments that form the basis of this study. Following this, a more detailed review of the modeling procedure is undertaken, along with a description of the fidelity assessment methodology. Next, the results of the flight test and simulation experiments

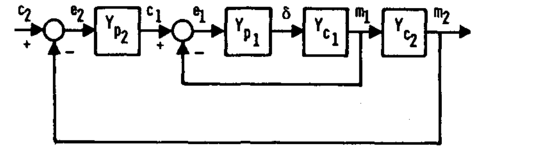

Fig. 1 Manual control task modeled with sequential loop closures.

Received Oct. 4, 1991; revision received Feb. 25, 1992; accepted for publication March 2, 1992.

*Professor, Department of Mechanical, Aeronautical and Materials Engineering. Associate Fellow AIAA.

†Graduate Student, Department of Mechanical, Aeronautical and Materials Engineering.

‡Aerospace Engineer, U.S. Army Aeroflightdynamics Directorate.

are presented, and the assessment procedure is exercised. Finally, after a discussion of the results, conclusions are drawn.

Flight and Simulation Experiments

The vehicle used in this study was the Army UH-60A Black Hawk, a twin-engine helicopter equipped with a single-main rotor. The test vehicle was instrumented so that, among other variables, linear velocities, angular rates and attitudes, and pilot control inputs could be recorded. In addition, a laser-tracking facility allowed vehicle position to be measured and recorded. The vehicle stability augmentation system was engaged during the tests; however, the flight path stabilization system was disengaged for the data analyzed here.

In this discussion, attention is focused on a single, well-defined flight task: a lateral side step maneuver, initiated from a stabilized hover near the ground. The side step maneuver was performed using an outside visual reference referred to as a hover test rig. This rig consisted of a beam slightly over 40 ft in length. For the lateral side step maneuver, the beam was suspended horizontally from a crane approximately 55 ft from the ground. At each end of the beam, separated by 40 ft, were a pair of targets, or hover boards, which provided precise visual cues to the pilot for the control of vertical, lateral, and longitudinal vehicle positions. Figure 2 shows the vehicle and hover test rig in the flight test.

The side step task description and performance requirements that follow resulted from discussions among NASA/Army researchers, including, of course, NASA test pilots. The side step task description is as follows:

Task: From a stabilized hover at the left hover board, rapidly translate to the right hover board and stabilize. Complete translation and stabilization within 7 s. Repeat maneuver to the left.

Performance (desired): With no objectional oscillations, maintain 1) altitude excursions within ±3 ft from the hover-board centerline throughout, and 2) heading excursions within ±5 deg of the desired heading, and 3) lateral excursions relative to the pilot's eyepoint, within the hover-board width, after stabilization.

Performance (adequate): Either 1) maintain desired performance using a time greater than 7 s to translate and stabilize, or 2) maintain desired performance for most of the task except for occasional stable excursions that exceed, but are followed by return to, desired performance limits.

Cooper-Harper pilot ratings[5] and associated pilot comments were recorded following each task. An additional questionnaire was employed to elicit pilot comments regarding specific handling qualities issues and simulation fidelity. During the conduct of the experiment four pilots participated in the task. However, because of simulation availability, only two of the pilots completed both flight test and simulation results. It should be noted that the time constraint in the task description just presented served as an *approximate* benchmark by which the pilots were asked to judge task completion performance. Pilots were not informed of side step completion times on every run, but they were given them if requested. Task initiation and completion (stabilization) were defined and called out by the evaluation pilot during each maneuver so that time performance could be monitored by the test personnel and the pilot could be informed if a violation occurred.

The simulation was conducted on the NASA Ames Vertical Motion Simulator. The visual scene was presented using a three-window cab with the computer-generated imagery (CGI) system with a centerline seating arrangement. By design, additional visual cues (i.e., those not derived from the test rig itself) were quite sparse in both the flight and the simulation experiments. The experiments were originally designed so that pilots typically could fly the vehicle and the simulator within the same week, often in the same day. However, a data recording failure in the simulation required a second simulator study to be conducted approximately five months after the original

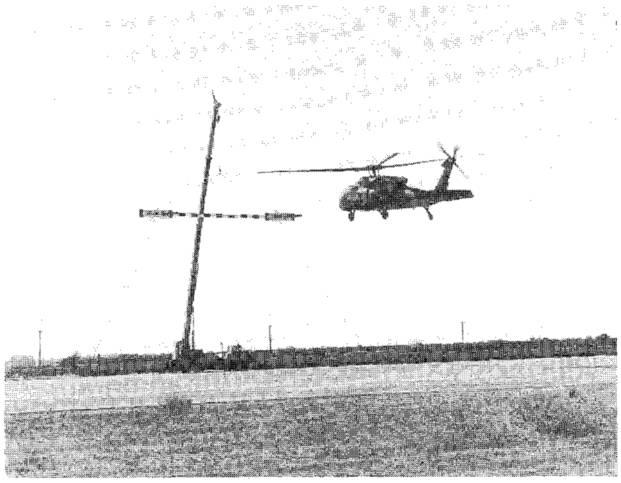

Fig. 2 Flight test hover rig.

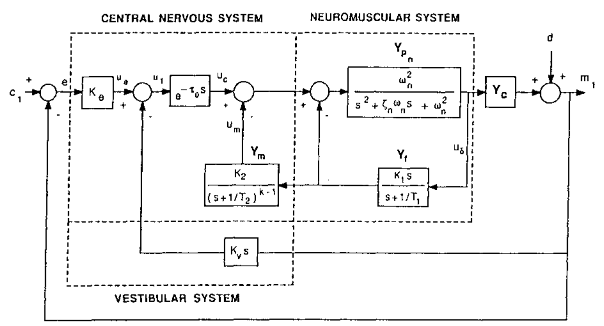

Fig. 3 Structural model of the human pilot.

experiments. It is this latter simulation effort that forms the basis of the fidelity assessment to be discussed.

Modeling Approach

Structural Model

The basic modeling approach that is used in the analytical portion of this study is presented in Ref. 1. The structural model of the human pilot,[6] shown in Fig. 3, is used to represent the pilot dynamics, including the effect of motion cues.[7] In an important extension of the work of Ref. 1, a handling qualities "sensitivity function" introduced in Ref. 8 is employed.

The model of Fig. 3 represents the pilot dynamics in the primary control loop, i.e., Yp_1 in Fig. 1. The model has been divided into central nervous system, neuromuscular system, and vestibular system components, a division intended to emphasize the nature of the signal processing activity involved. The system error e is presented to the pilot and multiplied by the gain K_e. If motion cues are available, output rate $\dot{m}_1$ is assumed to be sensed by the vestibular system (provided it is an angular velocity or linear or angular acceleration). The output rate is multiplied by the gain K_v and subtracted from the signal u_e. The resulting signal u_1 is passed through a central time delay τ_0 s, intended to account for latencies in the visual process sensing e, motor nerve conduction times, etc.

The signal u_c provides a command to a closed-loop system, which consists of a model of the open-loop neuromuscular dynamics Yp_n of the particular limb driving the manipulator (control stick, pedals, etc.) and elements Y_f and Y_m, which form two proprioceptive feedback loops in the structural model. It is this proprioceptive feedback, so-called because it is assumed to be derived from sensed manipulator position/force, which provides the basic equalization capabilities of the model and, by hypothesis, the human pilot. The form of Y_m is

Table 1 Nominal parameters for structural model

k	K_v	K_1	K_2	T_1, s	T_2, s	τ_0, s	ζ_n	ω_n, rad/s
0	0	1.0	2.0	5.0	—[a]	0.15	0.707	10.0
1	0	1.0	2.0	5.0	—[b]	0.15	0.707	10.0
2	0	1.0	10.0	2.5	—[a]	0.15	0.707	10.0

[a]Selected to achieve K/s-like crossover characteristics.
[b]Parameter not applicable.

Table 2 Cooper-Harper pilot rating summary

Pilot	Flight	Simulation
A	3.1[a]	4[b]
B	2[c]	4[d]

[a]Average of 10 ratings for 10 individual side steps.
[b]One rating for three double side steps.
[c]Average of seven ratings for seven individual side steps.
[d]One rating for four double side steps.

determined by the order k of the vehicle dynamics Y_c in the region of the crossover frequency ω_c.

Obviously, the structural model is not parsimonious in terms of the number of parameters involved. However, for the purposes of engineering analyses such as those that are the subject of the research to be described, experience has shown that the model parameters can be selected based on the characteristics of the vehicle dynamics near crossover and the necessity of the model's emulating the crossover model of the human operator.[9]

Structural Model Parameter Selection

The model parameter selection procedure is as follows[10]:

1) The flight task is analyzed and an appropriate feedback structure is selected, e.g., Fig. 1.

2) The vehicle transfer function Yc_1 for the primary control loop is obtained.

3) A primary-loop crossover frequency ω_c is estimated. The actual value of ω_c will be determined on the basis of desired gain and phase margins.

4) Given the primary-loop vehicle transfer function and the specified crossover frequency, the parameter k in the structural model of Fig. 3 is selected. The integer value of k will depend on whether gain ($k=1$), lead ($k=2$), or lag ($k=0$) equalization is required in the primary control loop, as dictated by the crossover model and the form of Y_c around the crossover frequency.

5) Given the value of k, the remaining structural model parameters, save T_2 and K_v, are selected from Table 1.

6) T_2 is chosen to ensure a K/s-like pilot-vehicle transfer function ($Yp_1 Y_c$) around crossover. Note that if $k=1$, T_2 is not utilized since the exponent on the factor $s+(1/T_2)$ in Y_m is $k-1=0$.

7) For application of the handling qualities assessment technique to be discussed, control system sensitivity must be eliminated as a variable in the modeling problem. To this end, adjust K_c, the "gain" of the controlled element, so that

$$K_c = \frac{1}{|Yp_1(j\omega)|_{\omega=\omega_c}|Y_c(j\omega)|_{\omega=\omega_c}} \tag{1}$$

Equation (1) ensures that the desired crossover frequency ω_c will be obtained, given the model parameter values of Table 1, with $K_e=1.0$ and $K_v=0$. The desired crossover frequency, in turn, is that value ensuring adequate gain margin (GM) and phase margin (PM) in the primary control loop. Here, ω_c is chosen to provide $GM=4$ dB and PM>45 deg, or $PM=45$ deg and $GM>4$ dB.

8) In the unlikely event that the crossover frequency of step 7 differs enough from that used in step 3 so that the order of the vehicle dynamics around crossover changes from that of step 3, repeat steps 3–8.

9) The motion cue feedback loop is now closed, and K_v is increased from zero until the minimum damping ratio of any complex root in the characteristic equation of the closed-loop m_1/c_1 transfer function equals a specified minimum value. The root locus technique is an obvious choice for accomplishing this task. A value of 0.15 for this damping ratio represents a tradeoff between stability and the high-frequency phase-lag reduction, which is hypothesized to constitute the primary dynamic benefit of motion feedback.[7]

10) Since the closure of the motion loop will affect the crossover frequency, steps 7–9 are repeated.

Although the procedure just outlined is iterative in nature, it can be accomplished quickly and efficiently using an interactive computer-aided control system design package.

Handling Qualities Sensitivity Function

It has been suggested by Smith[11] that, in any closed-loop tracking task, rate control activity on the part of the pilot is of fundamental importance from the standpoint of perceived handling qualities. For example, if the control task is pitch-attitude regulation in turbulence, pitch-rate control is the rate control activity in question. Smith held that a physiological measure for pilot option ratings is the rate at which nerve impulses (or an equivalent measure) arrive at the point within the central nervous system where all signals due to rate control are summed or operated upon.

Hess[10] has interpreted Smith's theory in terms of the structural model of Fig. 3 by showing that the signal u_m is proportional to vehicle output-rate due to control activity. In modeling a series of tasks for which simulation or flight test results were available in the form of HQRs, Hess showed that the mean square value of u_m, $\sigma^2_{u_m}$, which represents the average power in u_m, correlated quite well with HQRs; the larger the value of $\sigma^2_{u_m}$, the higher the HQR (the poorer the handling qualities).

Reference 8 carried this analysis a step further: Parseval's theorem shows that $\sigma^2_{u_m}$ can be expressed as

$$\sigma^2_{u_m} = \frac{1}{2\pi}\int_0^\infty \left|\frac{u_m}{c_1}(j\omega)\right|^2 \Phi_{cc}(\omega)\,d\omega \tag{2}$$

where $\Phi_{cc}(\omega)$ represents the power spectral density of the input c_1 to the primary control loop. The function $|u_m/c_1|$ is the magnitude of $u_m(j\omega)/c_1(j\omega)$ in Fig. 3. This function is called the handling qualities sensitivity function (HQSF) in Ref. 8. In Eq. (2), the HQSF can be thought of as a weighting function, determining how input power Φ_{cc} is transformed into rate-control power $\sigma^2_{u_m}$ by the human in the task at hand. One can see that the HQSF is dependent on all of the pilot-vehicle parameters of Fig. 3, i.e., Y_c and the elements Yp_n, Y_f, Y_m, etc. are all involved in the transfer function u_m/c_1.

Now the HQSF is so named because its Bode plot generally resembles that of the classical sensitivity function (the recipro-

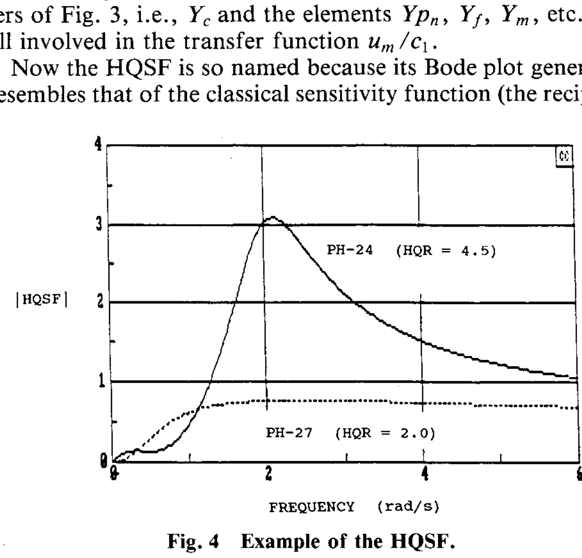

Fig. 4 Example of the HQSF.

cal of the return difference), i.e., low magnitude at frequencies below crossover and constant magnitude at frequencies above crossover. Since Φ_{cc} will be small beyond crossover, and since the HQSF is small below crossover, it is the crossover region alone that becomes critical in determining whether the HQSF is greater or less than unity.

As demonstrated in Ref. 8, the magnitude of the HQSF in the frequency range around ω_c can be used to delineate between level 1 ($HQR \leq 3.5$) and level 2 ($3.5 < HQR \leq 6.5$) handling qualities. Specifically, after modeling the pilot and task using the procedure outlined in the preceding section, if the magnitude of the HQSF just defined is less than (greater than) unity anywhere in the frequency range around crossover, then the vehicle and task will typically be rated as level 1 (level 2) by the pilot. Note that choosing $|HQSF| = 1.0$ as a dividing line between "satisfactory" (level 1) and "unsatisfactory" (level 2) handling qualities has a certain amount of face validity. At frequencies where $|HQSF| < 1.0$, Eq. (2) indicates that the HQSF is attenuating the contribution of Φ_{cc} to $\sigma^2_{u_m}$, whereas when $|HQSF| > 1.0$, the HQSF is magnifying the contribution of Φ_{cc} to $\sigma^2_{u_m}$.

As an example, consider a longitudinal helicopter hover task. This task was simulated in a fixed-based simulation study reported in Ref. 12. Figure 4 shows two HQSFs resulting from an application of the structural model to two vehicles with differing dynamics that were simulated in Ref. 12. Note that the Bode magnitude plots have been drawn with linear, as opposed to logarithmic, scales, since the integration implied by Eq. (2) is accomplished with respect to linear magnitude and frequency. Also shown in the figure are the average pilot ratings that the plots assigned. As the figure indicates, the HQSFs for PH-24 and PH-27 are larger than unity and smaller than unity, respectively, around the open-loop crossover frequency, which was approximately 3 rad/s. The assigned handling qualities levels are level 2 and level 1, respectively, for the vehicles in question.

It is the HQSF that will be called into service to extend the methodology introduced in Ref. 1 to allow a prediction of handling qualities levels in assessing simulator fidelity. Here one is not using the HQSF as a tool for investigating the handling qualities of the simulated vehicle per se, but rather one is investigating whether the HQSF of the simulated vehicle resembles that of the flight article. As mentioned in the preceding discussion, large differences in HQRs were noted in earlier flight test/simulation studies with the UH-60A. If such differences persist in the series of experiments that form the basis of this study, it definitely would be of interest to be able to trace their origins back to specific simulator characteristics or causes.

Results of Experiments and Analysis

Experiments

Table 2 summarizes the pilot rating results for the two pilots in the side step task for flight and simulation. As can be seen, the flight tasks fall in the level 1 area, whereas those in the simulator fall in the level 2 area.

The numerical ratings are supplemented by pilot comments, which are particularly informative in the simulation experiments, in that the pilots were specifically commenting on any disparities between simulation and flight. Examples follow.

Pilot A

"I'd say the most compensation in this task is in the roll axis.... There seems to be low roll damping, at least that's the perception from the cockpit, even though again I think it's probably a time delay.... There seemed to be a tendency for 'PIO' (pilot-induced oscillation) in the roll axis during the stabilization (phase of the task)... and the perception of low roll damping, which again may have been time delay .... Again, it's back to that perceived roll damping, which seems to be low in the simulation or which is more likely a time delay. If we can get that out of there and get the predictability of the roll up, that would increase the fidelity."

Pilot B

"The (yaw axis) is relatively slow. It eats up my time, so I never was really making the time criteria for this set of maneuvers. The airplane never felt like it was going to get away from me. It just takes longer to ... settle down.... Once you get over the right spot, (the control inputs required to maintain position are) fairly continuous, high frequency, but small. I would say that the roll (axis requires) the most compensation.... I would say there's no tendency to 'PIO,' mostly because of the lack of aggression in the task.... I probably couldn't have done it much quicker. The faster I tried to do it, the more difficulty I had stabilizing the airplane at the other end."

Figures 5 and 6 show representative time histories of side step maneuvers for pilot A in flight and in the simulator, respectively. Note that Fig. 5 (flight) is a right side step only, whereas Fig. 6 (simulation) shows both a right and a left side step. Scales are identical in Figs. 5 and 6 to allow easy comparison of the response magnitudes.

The roll rate and lateral cyclic input time histories indicate that pilot A typically used a more aggressive control strategy in the simulator than in flight. The opposite appeared to be the case for pilot B, where the more aggressive control activity appeared in flight. It was not felt that these differences were attributable to training effects, either in flight or simulation. The task and performance criteria were identical in both cases.

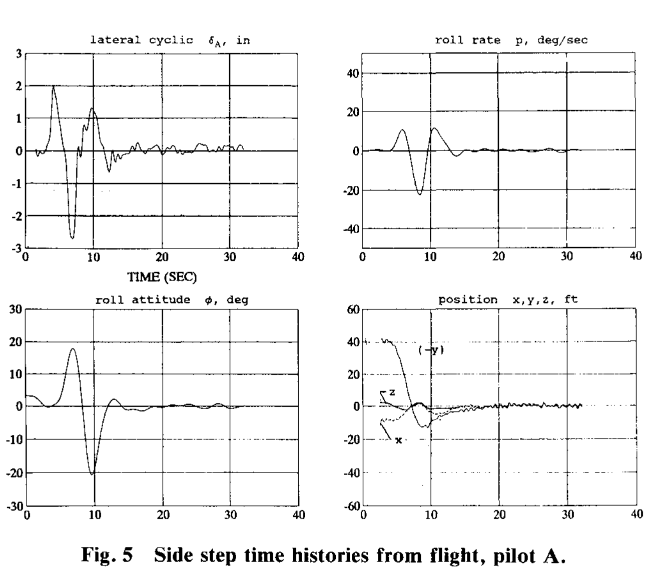

Fig. 5 Side step time histories from flight, pilot A.

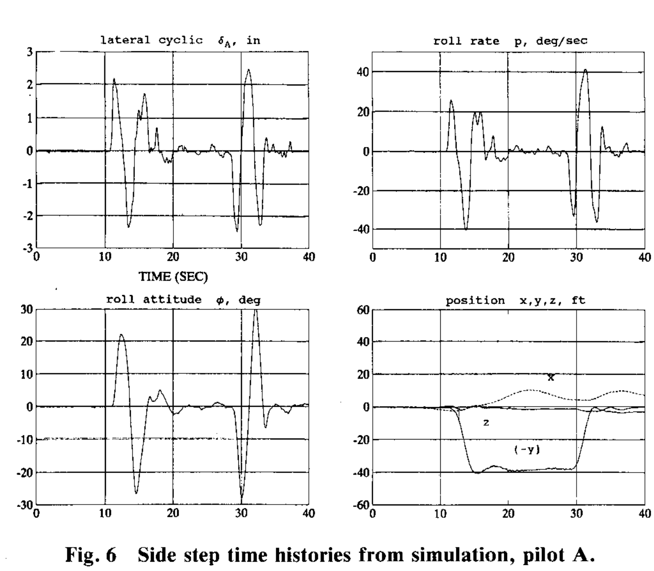

Fig. 6 Side step time histories from simulation, pilot A.

Table 3 Transfer function fits to hover frequency sweep measurements

Transfer function	Flight[a]	Simulator[a]
$\frac{\phi}{\delta_A}$ (rad/%)	$\frac{0.974e^{-0.0116s}}{(0.384)[0.392, 7.82]}$	$\frac{1.66}{(0.479)[0.535, 8.86]}$
$\frac{p_m}{\delta_A}\left(\frac{\text{rad/s}}{\%}\right)$	—	$\frac{0.0832(0)(0)e^{-0.133s}}{(0.956)(0.958)(11.9)(12.3)}$

[a]Rad and rad/s of attitude and rate per % of full travel of lateral cyclic stick; $(s+a_1)=(a_1)$, $(s^2+2\zeta_n\omega_n+\omega_n^2)=[\zeta_n,\omega_n]$.

Table 4 Modeling results; pilot/vehicle characteristics in primary control loop

Configuration	ω_c, rad/s	ω_b,[a] rad/s	ω_p,[b] rad/s	M_p,[c] dB
Flight	1.7	3.2	6.2	5.1
Simulation (As conducted)	1.2	1.7	1.5	2.9
Simulation (No CGI delay)	1.4	3.0	6.0	6.1
Simulation (Perfect motion)	1.5	2.4	2.3	5.4
Simulation (No motion)	1.4	2.1	2.0	6.4
Simulation (Modified dynamics)	1.5	2.3	2.2	3.9
Simulation (No CGI delay and perfect motion)	2.0	3.5	6.8	5.6

[a]Primary-loop bandwidth; frequency at which phase lag first reaches −90 deg.
[b]Primary-loop M peak frequency, frequency at which magnitude peak M_p occurs.
[c]Primary-loop magnitude peak.

Modeling

Figure 7 shows the pilot control strategy that was hypothesized for the side step maneuver.[1] Following the lead of Refs. 2 and 3 and the work of Ref. 1, the control strategy has been broken up into "rapid-response" and "error-reduction" phases. In the rapid-response phase, an open-loop roll-attitude input command is employed. This command, idealized as a doublet in Fig. 7, approximates a time optimal input to the system consisting of the dynamics y/ϕ_e. Time optimality is pertinent to this task, since the side step is time constrained and is intended to represent half of an "unmask-mask" type of maneuver often used in nap-of-the-Earth flight. In the error-reduction phase, an outer lateral position loop is assumed to be closed, which is used to create roll attitude commands. Although not employed here, the outer-loop compensation Yp_y is given by $Yp_y = K_y(T_L s + 1)$, i.e., a low-frequency lead term. Thus, in addition to lateral position, lateral translational rate is assumed to be used by the pilot.

In Fig. 7, the primary control loop is the innermost loop shown, i.e., that devoted to control of vehicle roll attitude. It is this loop that will be analyzed here. Thus, the error-reduction phase will not be modeled.

It is also assumed here that the roll attitude cues used in the primary control loop in simulator and flight are equivalent in terms of quality. As mentioned in the preceding discussion, the visual cues in flight were sparse in terms of texture and detail. In addition, considerable effort was directed toward reproducing the visual detail that was found in the hover test rig on the CGI display. Thus, in this analysis, it was felt that considering the only CGI limitation to be a time delay was valid. Of course, if one were modeling the error-reduction phase, a similar assumption would be more tenuous. There, precise translational rate and position information is needed, and one cannot so readily assume that the CGI presentation is equivalent in quality to flight.

The modeling procedure just outlined is begun by obtaining the pertinent vehicle transfer functions that will allow the pilot transfer function to be obtained for the primary control loop. This means obtaining the roll attitude (or roll rate) to lateral cyclic transfer function ϕ/δ_A for the vehicle in flight and in simulation. This was accomplished by employing a frequency sweep identification procedure discussed in Ref. 13.

The identification, conducted in flight and on the simulator, resulted in numerical data for the following frequency responses: p/δ_A (x body-axis component of vehicle angular velocity to lateral cyclic input) for flight and simulator, and p_m/δ_A (x body-axis component of simulator cab angular velocity to lateral cyclic input). In these definitions, the variable p represents 1) actual vehicle angular velocity in flight and 2) math model output in the simulator (not including CGI delay). The p_m/δ_A transfer function includes motion system washouts, gain attenuation, etc.

Transfer functions were then fit to the numerical frequency response data. In obtaining these fits, magnitude and phase data were limited to those that exhibited a linear coherence of approximately 0.80 or greater, which resulted in useable data over a frequency range of approximately 0.2–15 rad/s. Table 3 shows the resulting transfer function fits. Figure 8 is a comparison of the Bode plots for the fits shown in Table 3.

It is important to point out that the differences that one sees in the transfer function parameters in the first row of Table 3 are, of themselves, not necessarily indicative of simulator model inaccuracy. What may be important are the actual differences in the magnitudes and phases shown in Fig. 8. The fits of Table 3 merely allow the flight and simulation models to be represented by continuous transfer functions, rather than tabular data.

The measured frequency response data for the simulator did not include delays attributable to CGI scene generation. Although a delay compensation scheme was implemented and utilized in the simulation,[14] an estimated residual delay of 0.04 s remains even when the compensator is used. This value is used in the analysis as an additional delay in visual inputs to the pilot. This implies that a visual/motion cue mismatch existed in the simulator and was included in the modeling procedure.

With the transfer function data of Table 3, the modeling procedure followed the steps just outlined. The one addition to this procedure involved selection of the crossover frequency when the HQSF was being calculated. In obtaining the HQSF for different vehicle configurations involved in the same task, a common crossover frequency is used regardless of the gain and phase margins.[8,10] For this study, the flight crossover frequency was used in obtaining the HQSF for the simulation. The crossover frequency for flight was, however, obtained using the gain and phase margin criteria of step 7 of the modeling procedure. Thus, in modeling the simulation and *for the HQSF calculation alone*, the crossover frequency of step 7 in the modeling procedure was equated to that which resulted from modeling the flight task.

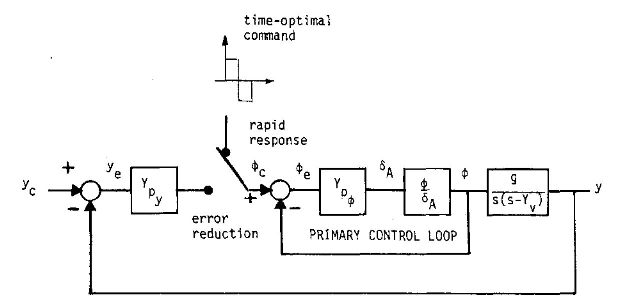

Fig. 7 Hypothesized pilot control strategy for side step maneuver.

After the modeling procedure is complete, a comparison of the resulting pilot/vehicle dynamics for flight and simulation is used to predict fidelity problems. This comparison involves the predicted pilot transfer functions around crossover, the closed-loop transfer functions of the primary control loop, and the HQSFs.

No fundamental differences in the predicted pilot transfer functions around crossover were encountered in the analysis. Table 4 compares the closed-loop frequency domain modeling results between flight and simulation for all but the HQSFs, which are better compared graphically. Included are a number of analytical variations of simulator characteristics. These are

1) An elimination of the 0.04 s CGI time delay.

2) The use of perfect motion cues, i.e., without washout and gain attenuation.

3) Fixed-base simulation (no motion).

4) Modified vehicle dynamics in the simulation (moving the quadratic pole at 8.86 to 20 rad/s to reduce the phase lags at high frequency).

5) The elimination of the CGI time delay and the use of perfect motion cues.

In addition to the pilot models for the flight and simulation (as conducted) configurations, each variation required generation of a new pilot model. Variation 4 deliberately introduces vehicle model errors in an attempt to compensate for the 0.04 s time delay. It should be emphasized that these variations were not actually evaluated in simulation. They only represent analytical variations in the model-based fidelity assessment technique. While elimination of motion constraints and time delays associated with visual scene generation may not be realistic alternatives for ground-based simulation, they do represent valid improvements that could be accomplished by in-flight simulation.

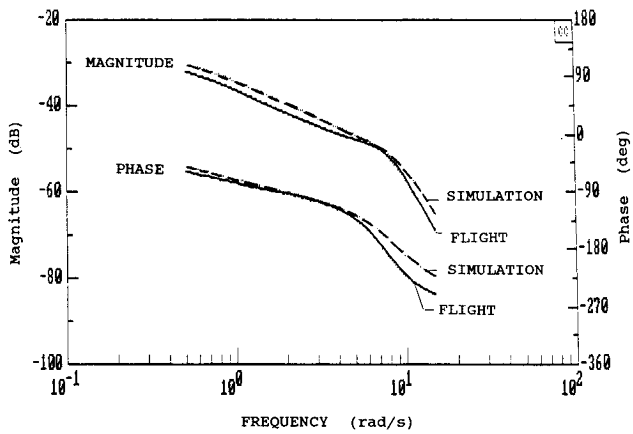

Fig. 8 Comparison of ϕ/δ_A transfer functions for simulation and flight. Simulation result does not include CGI delay.

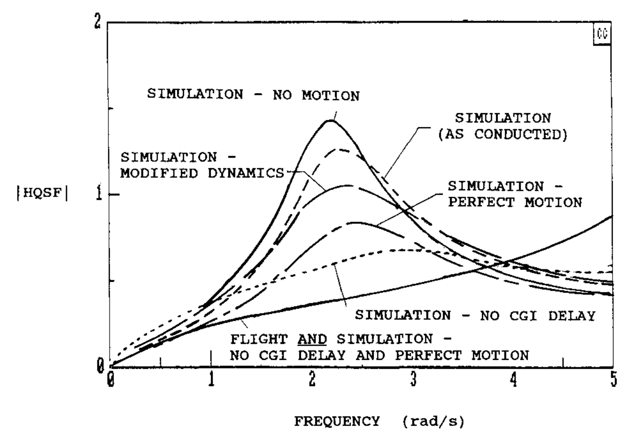

Fig. 9 HQSF comparison.

Reference 1 postulates that, in the absence of significant differences in predicted pilot transfer functions, the predicted closed-loop bandwidth ω_b between flight and simulation should differ by less than a factor of 1.5 for simulator fidelity problems attributable to the primary control loop to be absent. Table 4 indicates that the simulation (as conducted) fails to meet this criterion, whereas all of the analytical modifications except the no-motion case do. As pointed out in Ref. 1, the 1.5 factor is approximate, and it is intended to serve simply as a general guideline in the methodology.

Figure 9 compares the HQSFs of the configurations of Table 4. First note that, according to the HQSF criteria outlined in the preceding discussion, the simulation (as conducted) would be judged level 2 by the pilots and the flight would be judged level 1. This is because the HQSF for the simulation exceeds unity in the region of crossover, whereas that for flight remains well below unity in the same frequency range. This general result agrees with the HQR results shown in Table 2. In order of increasing similarity to the characteristics of the HQSF of the flight task, we have 1) the fixed-base (no motion) simulation, 2) the simulation (as conducted), 3) the simulation with modified dynamics, 4) the simulation with perfect motion, 5) the simulation with no CGI system delay, and 6) the simulation with no CGI system delay and perfect motion.

Again, according to the HQSF, the handling qualities of the first two configurations just mentioned would be judged as level 2 by the pilots, whereas those of the last three, including flight, would be judged as level 1. The simulation with modified dynamics would probably not allow such a definitive categorization, i.e., the HQSF is just slightly larger than unity. The lack of any significant differences in the HQSF for the simulation with no CGI delay and perfect motion and that of flight, and the similarity between the closed-loop characteristics of this configuration and flight (last and first rows of Table 4), suggest that the differences between the simulation math model and the dynamics of the flight vehicle shown in Table 3 and Fig. 8 have a minimal effect on simulation fidelity.

The addition of the HQSF to the fidelity assessment technique appears to complement the bandwidth (performance) criterion introduced in Ref. 1. Indeed, "similarity" in the overall shapes of the HQSFs between nominal and simulated vehicles and not just identical predicted handling qualities levels should probably be added as a criterion for simulation fidelity. In comparing nominal and simulated vehicles, the presence of such similarity would suggest similar relationships between the spectral characteristics of the primary loop command signal and rate-control activity (the hypothesized harbinger of handling qualities degradation). Of course, quantifying "similarity," like quantifying "significant" differences in bandwidth, can be somewhat difficult. The authors would argue that, in Fig. 9, the HQSF for the simulation with no CGI delay is the most "similar" to that for flight. Obviously, a mean square error could be defined between the HQSF for flight and that for any of the competing HQSFs in Fig. 9, although this was not done here.

Discussion

The pilot ratings and comments indicate that fidelity problems exist in the simulation of the side step maneuver. The modeling results predict fidelity problems and point to the CGI time delay as a major contributor. However, motion system limitations also contribute to the problem. The first two rows of Table 4, indicating a reduced primary control-loop bandwidth in simulation as compared to flight, would predict differences in control aggressiveness between simulation and flight akin to those exhibited by pilot B, but not by pilot A. This inconsistency does not necessarily imply a modeling problem. The performance assessment part of the modeling procedure required minimum stability margins to be in evidence. Pilot A apparently adopted a control strategy that resulted in relatively small stability margins, e.g., recall his comments regarding the PIO susceptibility of the simulation. The modeling procedure outlined here and in Ref. 1 is not intended to account for control strategy differences between two pilots flying the same vehicle, whether in flight or simulation.

The introduction and use of the HQSF represents a significant extension of the modeling procedure discussed in Ref. 1. The HQSF can present a useful picture of how changes in simulation characteristics would affect fidelity, as reflected in perceived handling qualities.

The ability of a modification in the simulated vehicle dynamics to enhance simulation fidelity as predicted by the modeling procedure may appear somewhat contradictory. What was done, of course, was to trade some magnitude distortion in the vehicle dynamics associated with the primary control loop for decreased phase lags. These decreased lags, in turn, compensated somewhat for the CGI time delay. Although the variation included in the modeling study was somewhat crude, it does indicate that some benefits may accrue from this approach, particularly in reducing those residual delays that remain after other delay compensation techniques are in use. One way to include such a variation in the simulator, for example, is to increase the bandwidths of the control actuators modeled in the simulation.

Conclusions

1) A simulator fidelity assessment scheme previously discussed in the literature has been extended to include the use of a handling qualities sensitivity function.

2) Flight test and simulation experiments have indicated the existence of simulation fidelity problems in a low-altitude lateral translational maneuvering task (side step) of a UH-60A rotorcraft.

3) The analytical fidelity assessment scheme and, in particular, the handling qualities sensitivity function, indicated that visual scene time delays make a major contribution to the fidelity problem, with motion system characteristics also playing a significant role.

Acknowledgment

This research was supported by Grant NAG 2-482 from the U.S. Army Aeroflightdynamics Directorate, NASA Ames Research Center, Moffett Field, California. Adolph Atencio Jr. was the contract technical manager.

References

[1]Hess, R. A., and Malsbury, T., "Closed-Loop Assessment of Flight Simulator Fidelity," *Journal of Guidance, Control, and Dynamics,* Vol. 14, No. 1, 1991, pp. 191–197.

[2]Ferguson, S. W., Clement, W. F., Cleveland, W. B., and Key, D. L., "Assessment of Simulation Fidelity Using Measurements of Piloting Technique in Flight," American Helicopter Society, Paper A-84-40-08-4000, May 1984.

[3]Ferguson, S. W., Clement, W. F., Hoh, R. H., and Cleveland, W. B., "Assessment of Simulation Fidelity Using Measurements of Piloting Technique in Flight, Part II," 41st Annual American Helicopter Society Forum, May 1985.

[4]Hess, R. A., "Feedback Control Models," *Handbook of Human Factors,* Wiley, New York, 1987, Chap. 9.5, pp. 1212–1242.

[5]Cooper, G. C., and Harper, R. P., "The Use of Pilot Rating in the Evaluation of Aircraft Handling Qualities," NASA TN D-5153, April 1969.

[6]Hess, R. A., "A Model-Based Theory for Analyzing Human Control Behavior," *Advances in Man-Machine Systems Research,* edited by W. B. Rouse, Vol. 2, JAI Press, London, 1985, pp. 129–176.

[7]Hess, R. A., "A Model for the Human's Use of Motion Cues in Vehicular Control," *Journal of Guidance, Control, and Dynamics,* Vol. 13, No. 2, 1990, pp. 476–482.

[8]Hess, R. A., and Yousefpor, M., "Analyzing the Flared Landing Task with Pitch-Rate Flight Control Systems," *Journal of Guidance, Control, and Dynamics,* Vol. 15, No. 3, 1992, pp. 768–774.

[9]McRuer, D. T., and Krendel, E. S., "Mathematical Models of Human Pilot Behavior," AGARDograph 188, 1974.

[10]Hess, R. A., "A Theory for Aircraft Handling Qualities Based Upon a Structural Pilot Model," *Journal of Guidance, Control, and Dynamics,* Vol. 12, No. 6, 1989, pp. 792–797.

[11]Smith, R. H., "A Unifying Theory for Pilot Opinion Rating," *Proceedings of the 12th Annual Conference on Manual Control,* NASA TM X-73,170, May 1976, pp. 542–558.

[12]Miller, D. P., and Vinje, E. W., "Fixed-Base Simulator Studies of VTOL Aircraft Handling Qualities in Hovering and Low Speed Flight," Air Force Flight Dynamics Lab., AFFDL-TR-67-152, Wright-Patterson AFB, OH, Jan. 1966.

[13]Tischler, M. B., "System Identification Requirements for High-Bandwidth Rotorcraft Flight Control System Design," *Journal of Guidance, Control, and Dynamics,* Vol. 13, No. 5, 1990, pp. 835–841.

[14]McFarland, R. E., "CGI Delay Compensation," NASA Ames Research Center, NASA TM 86703, Moffett Field, CA, Jan. 1986.